J Mater Sci (2008) 43:7432–7437
DOI 10.1007/s10853-008-2871-z

ULTRAFINE-GRAINED MATERIALS

Flow properties of an aluminum alloy processed by equal channel angular pressing

A. Sivaraman · Uday Chakkingal

Received: 9 March 2008 / Accepted: 9 July 2008 / Published online: 9 August 2008

Abstract Equal Channel Angular Pressing (ECAP) process is an important process for producing ultrafine-grained microstructures in bulk metals and alloys. In the present work, aluminum alloy AA 6063 samples were subjected to ECAP for up to three passes using an ECAP die with a die angle of 105°. The strain imparted to the specimen after three passes was approximately 2.64. Compression testing of the ECAP specimens was carried out to determine the subsequent flow behavior. Two types of compression test specimen orientations, one parallel to the axis of pressed sample and the other at 45° to the axis of the pressed sample, were used for the study. The strain path change (SPC) parameter was used to quantify the strain path change involved in straining by ECAP followed by straining by uniaxial compression. Higher flow strength values were observed in compression in specimens machined at 45° to the axis of the ECAP specimens. Flow softening and anisotropic behavior have been studied with respect to the number of passes and processing routes.

Introduction

Equal channel angular pressing is a severe plastic deformation technique (SPD) used to impart a large amount of plastic strain to bulk metallic materials [1]. This technique is capable of producing large fully dense samples containing an ultrafine grain size in the submicrometer or nanometer range [2]. A special die, which consists of two channels of identical cross section intersecting at an angle 2ϕ, is used for this purpose. Basically the specimen is pressed from one channel to the next by a punch; ideally deformation takes place by shear at the intersecting plane. A schematic of the ECAP die setup is shown in Fig. 1. Different processing routes can be used for the deformation. Route *A*—orientation of the specimen remains unchanged for consecutive passes, Route *C*—the specimen is rotated by 180° for consecutive passes, etc. [3, 4]. The equivalent plastic strain per pass under ideal simple shear conditions is given by [1]

$$\varepsilon = (2/\sqrt{3})\cot\phi \tag{1}$$

where 2ϕ is the included angle.

The ultrafine grained (UFG) microstructures developed after ECAP represent high-energy configurations. The UFG microstructure consists of cell blocks and subgrains separated by low-angle grain boundaries and a significant fraction of high-angle grain boundaries. The dislocation density is also high, and the dislocations appear as dislocation tangles and dislocation pileups at grain boundaries. Therefore, as a result of change in loading or strain path during subsequent deformation, the UFG microstructure may be unstable resulting in effects like flow softening. This has been investigated in the current study by subjecting ECAP specimens to further deformation by uniaxial compression along two different strain paths. To vary the strain path, compression test specimens were machined in two orientations: with compression axis parallel to the ECAP direction and at 45° to the ECAP direction.

The magnitude of strain path change (SPC) can be quantified using the parameter θ, originally proposed by Schmitt et al. [5]. SPC parameter is defined as the scalar product of the two successive (normalized or unit) strain

A. Sivaraman (✉) · U. Chakkingal
Materials Forming Laboratory, Department of Metallurgical and Materials Engineering, Indian Institute of Technology Madras, Chennai 600 036, India
e-mail: sengiram2k2@yahoo.co.in

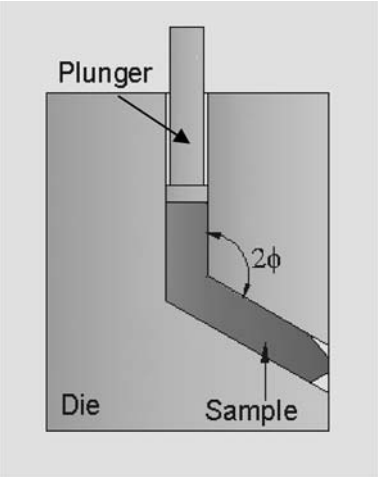

Fig. 1 ECAP Die setup

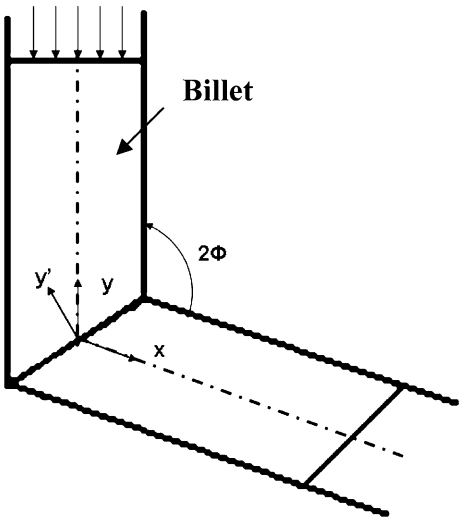

Fig. 2 Co-ordinate system used to designate geometry of compression specimens and the strain path during uniaxial compression

rate tensors [5–7]. Based on the θ value, the magnitude of strain path change can be identified. Generally SPC parameter θ can vary between $+1$ and -1. A value of 1 corresponds to no change in strain path, i.e., monotonic loading. A value of -1 can be taken as complete reversal of the strain path during subsequent straining. This is said to be Bauschinger type loading. A value of 0 corresponds to orthogonal loading. The flow properties and microstructure have been interpreted on the basis of the strain path change (SPC) parameter, θ.

Similar experiments were conducted by Sivaraman et al. [8] for commercial pure Al subjected to ECAP in a 90° die. It was observed that strain path change has a significant effect on flow properties of the material. In the current study, the effect of strain path change on a commercially significant aluminum alloy AA6063 subjected to ECAP using a 105° die has been investigated.

Experimental procedures

The experiments were conducted on aluminum alloy AA6063. The initial material was solutionized at 520 °C for 2 h and quenched in water. Cylindrical specimens 20 mm in diameter and 110 mm length were used for ECAP. The ECAP die was designed with an angle 2ϕ of 105°. The equivalent plastic strain imparted in each pass was approximately 0.88. ECAP was conducted on aluminum alloy specimens for up to three passes for both route *A* and route *C*. The total strain after three passes was therefore approximately 2.64. Two different types of compression specimens were prepared from the specimens pressed after ECAP: one with axis parallel (x direction) to the ECAP pressing direction and the other with axis inclined at 45° (y' direction) to the pressing direction. (Refer Fig. 2 for the co-ordinate system used.) This was done to study the influence of changing strain path on microstructure and mechanical properties. The ECAP specimens were machined to produce compression test specimens 8 mm in diameter and 10 mm in height so that the aspect ratio (ratio of height to diameter) of the specimen was 1.25. Compression tests were conducted on these specimens using MoS_2 as the lubricant. The initial strain rate during compression was approximately 0.02 s^{-1}. For each condition three specimens were tested. All the specimens were compressed to a strain of approximately 0.8 at room temperature. Force-stroke data were recorded using a data acquisition system during the test. True stress-true strain curves were plotted and fitted to the power law equation of the form

$$\sigma = K\varepsilon^n \tag{2}$$

where K is the strength coefficient and n is the strain hardening exponent.

TEM observations were made to characterize the microstructures after ECAP and after ECAP + compression. TEM samples were taken from central portion of the ECAP-processed specimens. The thickness of the TEM specimen was reduced by mechanical grinding. Twin jet electro polishing was done in an electrolytic solution consisting of 20% of perchloric acid and 80% of ethanol at a temperature of -20 °C and a voltage of 15 V. The foils obtained after electro polishing were used for the TEM studies.

Results and discussion

Figure 3 shows the flow curves of specimens compressed in both x and y' directions after deformation by ECAP. The

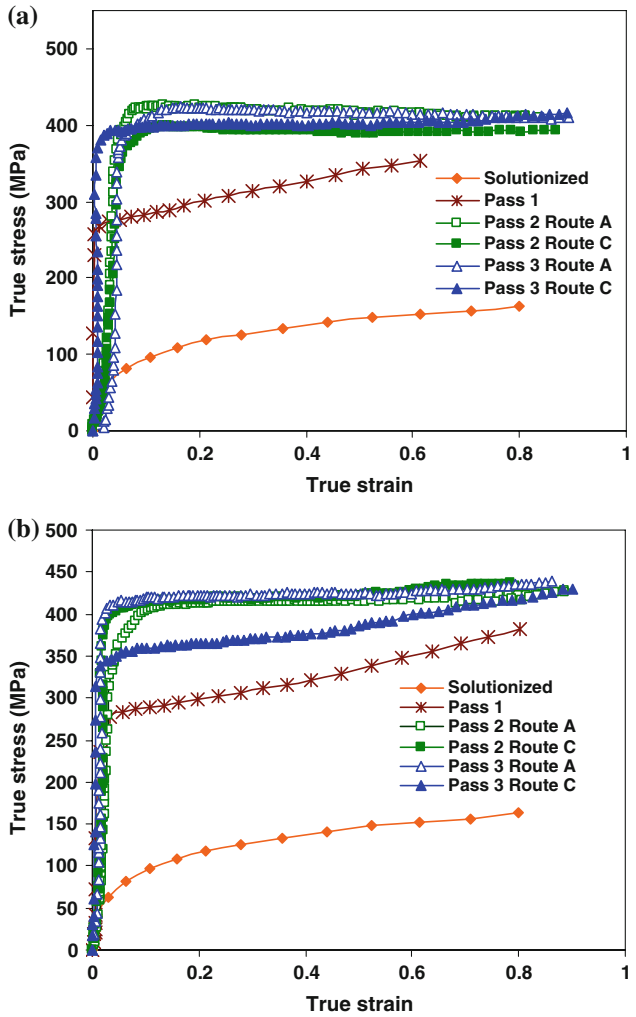

Fig. 3 Flow curves of ECA-pressed specimens (**a**) compressed in x direction (**b**) and compressed in y' direction

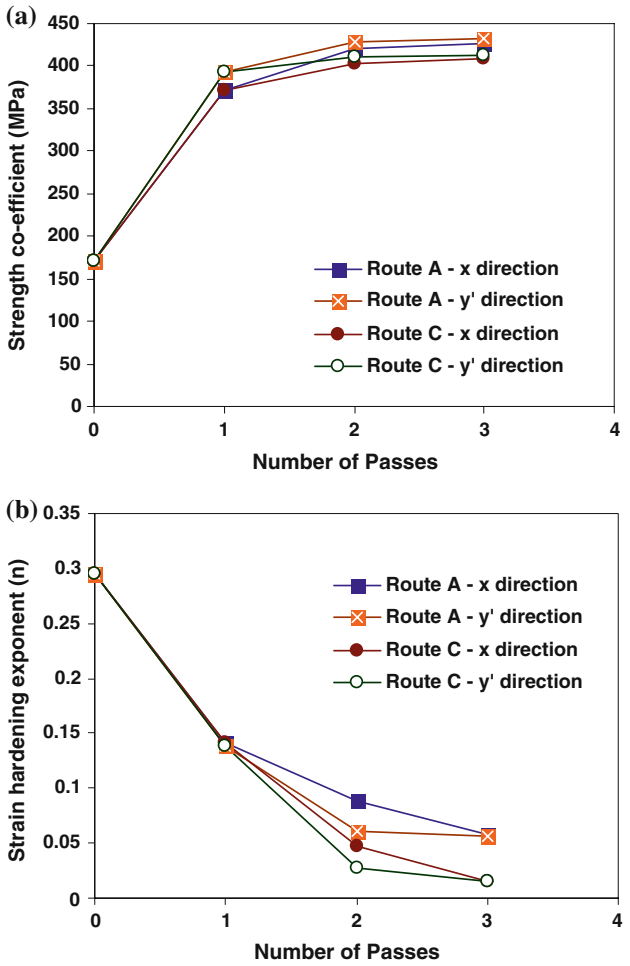

Fig. 4 Variation of (**a**) Strength coefficient and (**b**) Strain hardening exponent values with respect to number of passes

solutionized specimens and specimens after first pass exhibit strain hardening. However, specimens after second and third passes of ECAP exhibit very little strain hardening. The values of the strength coefficient, K, and the strain hardening exponent, n, extracted from the flow stress data are given in Fig. 4a, b. The K and n values of solutionized material were found to be 170 MPa and 0.295, respectively. After ECAP by Route A, the values of K increased up to three passes; however, n values kept decreasing with respect to increase in number of passes. From the results it is found that the flow strength values in the y' direction are higher compared to values in the x direction. For example, after first pass the K value was found to be 371 MPa in x direction but in the case of y' direction it was 393 MPa. Similar results were observed for all the passes. After second pass by Route A, K and n were determined to be 421 MPa and 0.088 for specimens compressed in the x direction and 425 MPa and 0.061 for specimens at 45° to the ECAP direction (y' direction). After three passes by Route A, K and n were determined to be 426 MPa and 0.058 for specimens compressed in the x direction, and 432 MPa and 0.056 for specimens compressed in the y' direction. After second pass by Route C, K and n were determined to be 403 MPa and 0.0477 for specimens compressed in x direction and 410 MPa and 0.028 for specimens at 45° to the ECAP direction (y' direction). After third pass the K and n values were 409 MPa and 0.016 for x direction, and in the case of y' direction the values were 413 MPa and 0.015. For both processing routes A and C, higher values of K were observed for compression specimens at 45° to the ECAP direction compared to specimens parallel to the ECAP direction. This implies that the direction of the straining after ECAP influences the flow behavior.

The flow strength of the material for a strain of 0.1 is shown in Fig. 5. It is observed that the flow strength values are somewhat higher in the case of compression specimens at 45° to the ECAP direction compared to compression

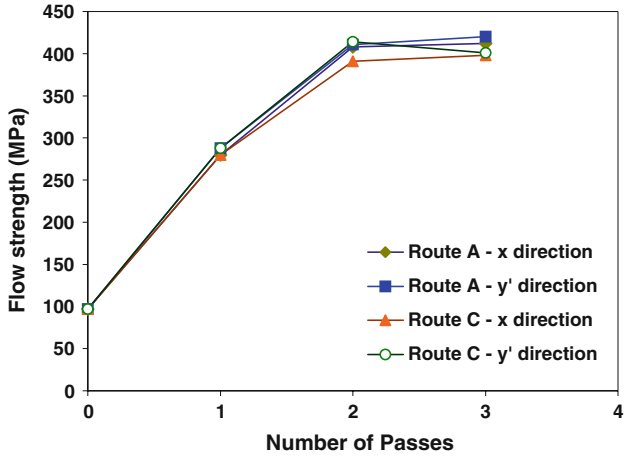

Fig. 5 Flow strength values at a strain of 0.1 from compression test after ECAP

specimens parallel to the ECAP direction which is similar to the results of strength coefficient values.

These data can be interpreted and understood on the basis of the strain path change (SPC) parameter, θ. The SPC parameter for ECAP followed by compression in the x direction has been reported to be $-(\sqrt{3}/2)\sin(2\phi)$ by Li [7]. This gives a θ value of -0.83 for ECAP with a die angle $2\phi = 105°$. The SPC parameter, θ, for ECAP followed by compression in the y' direction sequence can be calculated using the appropriate strain rate equation [6, 7].

$$\theta = \cos\alpha = A^{(1)} : A^{(3)} = \frac{\dot{\varepsilon}^{(1)}}{\sqrt{\dot{\varepsilon}^{(1)} : \dot{\varepsilon}^{(1)}}} : \frac{\dot{\varepsilon}^{(3)}}{\sqrt{\dot{\varepsilon}^{(3)} : \dot{\varepsilon}^{(3)}}} \tag{3}$$

where $A^{(1)}$ and $A^{(3)}$ are the unit vectors in the strain rate space associated with $\dot{\varepsilon}^{(1)}$ and $\dot{\varepsilon}^{(3)}$, the strain rate tensors associated with the first and second deformation stages, respectively. α represents the angle between the vectors representing the first deformation (by ECAP) and the second deformation (by compression). The value of the SPC parameter, θ, can in principle be calculated using the two normal strain ε_{xx} values. According to Dupuy et al. [9], ECAP involves very large strains and therefore it may be necessary to use Lagrangian definitions of strain instead of an Eulerian definition. They suggest an easier alternative to calculate the SPC is to define it in terms of strain rate tensors. This approach has been used in this paper.

For ECAP, the unit vector in strain rate space is given by Li [7] as

$$A^{(1)}_{xyz} = \frac{1}{\sqrt{2}}\begin{bmatrix} \sin 2\phi & -\cos 2\phi & 0 \\ -\cos 2\phi & \sin 2\phi & 0 \\ 0 & 0 & 0 \end{bmatrix} \tag{4}$$

The strain rate tensor associated with the compression in the 45° orientation is given by

$$\dot{\varepsilon}^{(3)}_{xyz} = \begin{bmatrix} \frac{\dot{\varepsilon}_{xx}+\dot{\varepsilon}_{yy}}{2} & \frac{\dot{\varepsilon}_{xx}-\dot{\varepsilon}_{yy}}{2} & 0 \\ \frac{\dot{\varepsilon}_{xx}-\dot{\varepsilon}_{yy}}{2} & \frac{\dot{\varepsilon}_{xx}+\dot{\varepsilon}_{yy}}{2} & 0 \\ 0 & 0 & \dot{\varepsilon}_{zz} \end{bmatrix} \tag{5}$$

where, $\dot{\varepsilon}_{xx}$, $\dot{\varepsilon}_{yy}$ and $\dot{\varepsilon}_{zz}$ are the principle strain rates along the x, y, and z axes, respectively. Then the unit vector in strain rate space for compression in y' direction is given by Eq. 6 below.

$$A^{(3)}_{xyz} = \frac{1}{\sqrt{\frac{\left[\dot{\varepsilon}_{xx}+\dot{\varepsilon}_{yy}\right]^2}{2} + \frac{\left[\dot{\varepsilon}_{xx}-\dot{\varepsilon}_{yy}\right]^2}{2} + \dot{\varepsilon}^2_{zz}}} \begin{bmatrix} \frac{\dot{\varepsilon}_{xx}+\dot{\varepsilon}_{yy}}{2} & \frac{\dot{\varepsilon}_{xx}-\dot{\varepsilon}_{yy}}{2} & 0 \\ \frac{\dot{\varepsilon}_{xx}-\dot{\varepsilon}_{yy}}{2} & \frac{\dot{\varepsilon}_{xx}+\dot{\varepsilon}_{yy}}{2} & 0 \\ 0 & 0 & \dot{\varepsilon}_{zz} \end{bmatrix} \tag{6}$$

Now the strain path change parameter, θ, can be calculated as

$$\theta = \cos\alpha = A^{(1)} : A^{(3)}$$

The SPC parameter for ECAP followed by compression in the y' direction can be found from the following equation [9]

$$\theta = \frac{(-3/2)\,\varepsilon_{xx}\cos 2\phi}{\sqrt{3}|\varepsilon_{xx}|} \tag{7}$$

Since the ECAP die angle used in the current study is 105°, the SPC parameter (θ) for ECAP followed by compression in y' direction is equal to 0.22. A value of $\theta = 1$ corresponds to no change in strain path; a value of $\theta = -1$ corresponds to completely reversed straining while a value of $\theta = 0$ corresponds to orthogonal loading. Therefore there is larger amount of strain reversal when ECAP specimens are further strained by compression in the x direction. As per the work of Dupuy et al. [9], route C always promotes strain reversal and the value of SPC parameter equals -1, and for Route A processing with a 105° die as used in this study, the value of the SPC is -0.88. Therefore between successive ECAP passes also there is a significant amount of strain reversal (which can be considered to be nearly identical, as the SPC values are very close). In the current study, what is investigated is the effect of strain path change between the last ECAP pass and the subsequent deformation step by compression.

In the present study, the reloading direction is different for each case since it involves two different routes and three passes of ECAP (during pre-strain) followed by compression. Between the routes A and C, route A exhibits higher values of flow stress. There is a reduction in work hardening rate after first pass. The reduction in flow strength values in the x direction is expected because strain reversal leads to flow softening. During ECAP, dislocations form dislocation tangles, cell walls and subgrain boundaries whose configuration and distribution depend upon the

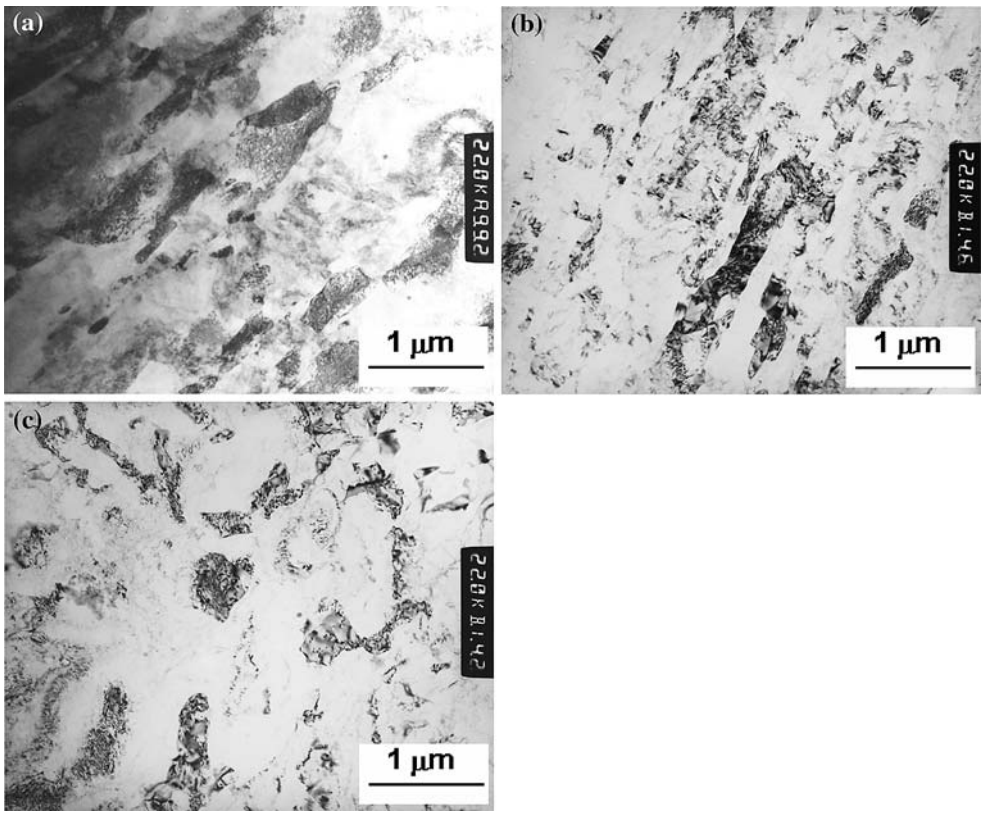

Fig. 6 TEM microstructures of (**a**) 3rd pass route *A* (**b**) 3rd pass route *A* followed bycompression in *x* direction and (**c**) 3rd pass route *A* followed by compression in y' direction

processing route used. When the strain is reversed, dislocations and cell walls can be annihilated and this leads to reduction in flow strength of the material. This is more likely to happen in compression in *x* direction as the θ value is closer to -1 (which corresponds to completely reversed straining). In the y' direction, the value of θ is close to zero. This strain path change implies that deformation has to take place by slip on slip systems, which were inactive during the ECAP. This gives rise to strengthening during orthogonal SPC resulting in an increase in the flow strength of the material. This is evident from the *K* values obtained from compression tests.

The microstructures of specimens after 3rd pass of route *A* followed by compression in *x* and y' direction is shown in Fig. 6. The microstructure after 3rd pass of route A mainly consists of elongated band structure with lamellar grain boundaries with high dislocation density. The material compressed in *x* direction after ECAP does not reveal a significant change in the microstructure. In this case the same slip systems may be active; only the direction of straining changes. But the microstructure of the material compressed in the y' direction no longer shows the banded microstructure resulting from ECAP due to the activation of new slip systems. When the strain path change is nearly orthogonal, i.e., subsequent straining is nearly at 90° to the initial straining, it is expected that Schmid factor values will not favor the initial slip systems leading to activation of previously inactive slip systems. Similar results were observed after 3rd pass of route *C* (Fig. 7).

These results have significance in the usage of ultrafine grained-materials in industrial applications. A basic conclusion is that there is anisotropy in mechanical properties. Secondly, since the flow properties are dependent upon the orientation of subsequent straining, loading in some orientations may even lead to flow softening.

Summary

The effect of change in strain path on the flow properties of aluminum alloy 6063 after ECAP using a 105° angle die has been investigated using compression testing on specimens oriented parallel to ECAP direction and at 45° to the ECAP direction. These correspond to two different strain path change parameters: -0.83 for parallel (near reversal of strain path) and 0.22 for 45° orientation (near orthogonal change in strain path). Specimens subjected to one ECAP pass exhibit significant strain hardening; however, after two passes very little strain hardening is observed irrespective of the processing route and compression specimen

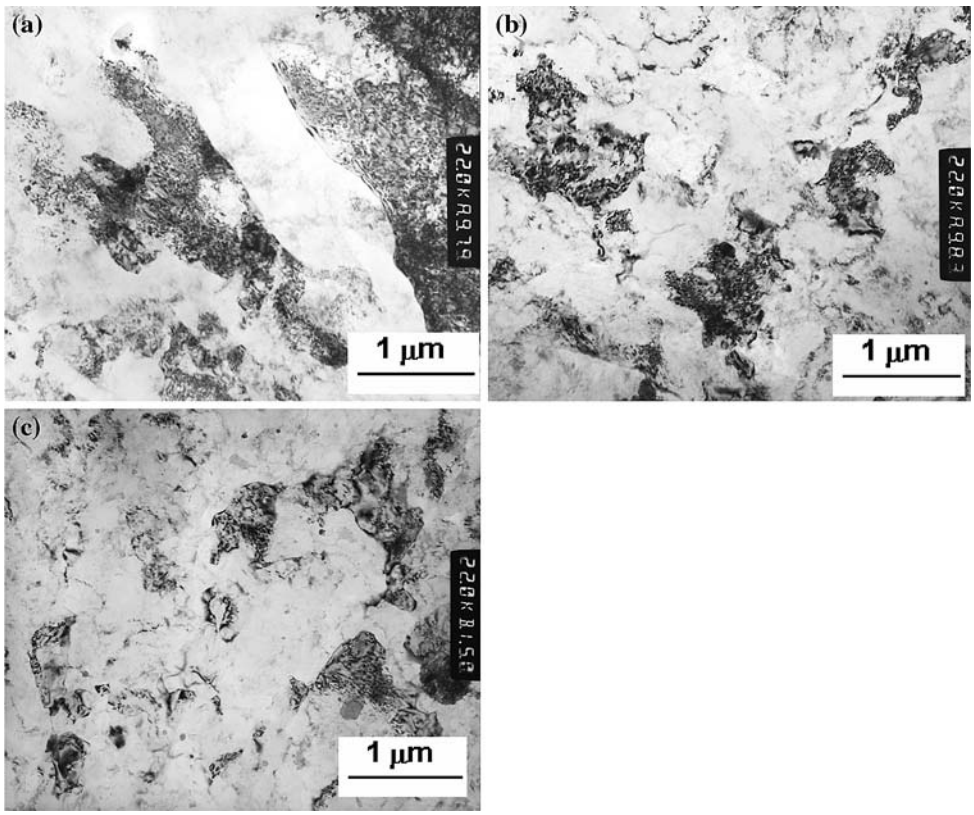

Fig. 7 TEM Microstructures of (**a**) 3rd pass route *C* (**b**) 3rd pass route *C* followed by compression in *x* direction and (**c**) 3rd pass route *C* followed by compression in *y*′ direction

orientation. Higher strength values were obtained after compression in the 45° orientation. The microstructures after ECAP and after compression along ECAP axis do not show any significant change. However compression at 45° to the ECAP direction leads to the formation of new microstructures. The flow properties after ECAP are therefore dependent on the subsequent strain path.

Acknowledgement This work was supported through a project sponsored by the Naval Research Board, Government of India, New Delhi. This support is gratefully acknowledged.

References

1. Segal VM (1995) Mater Sci Eng A 197:157–164. doi:10.1016/0921-5093(95)09705-8
2. Valiev RZ, Mulyukov RR, Ovchinnikov VV, Shabashov VA (1991) Scr Metall Mater 25:2717. doi:10.1016/0956-716X(91)90145-Q
3. Segal VM (1999) Mater Sci Eng A 271:322–333. doi:10.1016/S0921-5093(99)00248-8
4. Valiev RZ, Langdon TG (2006) Prog Mater Sci 51:881–981. doi:10.1016/j.pmatsci.2006.02.003
5. Schmitt JH, Fernandes JV, Gracio JJ, Vieira MF (1991) Mater Sci Eng A . doi:10.1016/0921-5093(91)90840-J
6. Sakharova NA, Fernandes JV (2006) Mater Chem Phys 98:44–50. doi:10.1016/j.matchemphys.2006.01.038
7. Li S (2007) Scr Mater 56:445–448. doi:10.1016/j.scriptamat.2006.12.006
8. Sivaraman A, Chakkingal U (2008) Mater Sci Eng A 487:264
9. Dupuy L, Rauch EF (2002) Mater Sci Eng A 337:241